Grzegorz KOSZAŁKA
Mirosław GUZIK
Andrzej NIEWCZAS

PTNSS–2011–SC–061

Numerical simulation of the ring twists during diesel engine operation

Abstract: The paper presents a mathematical model of ring pack of a diesel engine. A submodel of ring twists is described in details. Numerical algorithms applied and computer program worked out are characterised. A method of input data determination and results of simulations are also described. The results of initial simulations investigating the effect of engine operation condition on ring twists are pesented. The possible applications of the results of calculations in engine design is also discussed in the paper.

Key words: *diesel engine, ring-pack, ring twist, blowby, oil film*

Symulacyjne badania skręceń pierścieni uszczelniających podczas pracy sinika ZS

Streszczenie: W artykule przedstawiono matematyczny model uszczelnienia tłok-pierścienie-cylinder silnika spalinowego o zapłonie samoczynnym, w szczególności podmodel opisujący skręcenia pierścieni tłokowych. Scharakteryzowano założenia modelu oraz opracowaną aplikację komputerową. Opisano sposób wyznaczania danych wejściowych oraz przedstawiono wyniki wstępnych badań wpływu warunków pracy silnika na skręcenia pierścieni. Omówiono możliwe obszary wykorzystania wyników badań symulacyjnych prowadzonych z wykorzystanie opracowanego programu komputerowego.

Słowa kluczowe: *silnik ZS, uszczelnienie pierścieniowe, skręcenia pierścieni, przedmuchy spalin, film olejowy*

1. Introduction

The main function of the piston-rings-cylinder (PRC) assembly in a diesel engine is to seal the combustion chamber in a tight manner. In order to ensure the proper functioning of the seal, the rings must have the opportunity to move in the piston ring grooves, thus they need to be clearance fitted. Ring clearances in the grooves make the rings not only move along the groves, but also twist during engine operation. This movements have a significant influence on the gas flow through the PRC assembly and the formation of oil film between rings and cylinder, therefore on the efficiency, durability and reliability of an engine. In extreme cases, the phenomenon of ring twists may result in their breaking during engine operation. Experimental investigation of the twist angle is presently extremely difficult for technical reasons. However, due to simulation analyses, these phenomena may be investigated on the basis of appropriate numerical models. This paper presents a mathematical model of ring twists and a computer program designed on the basis of this model as well as the results of initial calculations.

2. Mathematical model

The model assumes that the rings, piston and cylinder are symmetrical to the main axis of the cylinder. Due to this, geometric model can be examined as flat, i.e. defined with two coordinates: axial and radial. Such assumption is often accepted [2, 3, 5, 8, 10, 11].

In order to calculate the twist angle α of the ring, it is necessary to determine the forces acting on the ring and the moments of these forces (Fig. 1). The system is established under the condition of the balance of axial and radial forces and their moments

$$\sum F_x = 0, \quad \sum F_y = 0, \quad \sum M = 0 . \qquad (1)$$

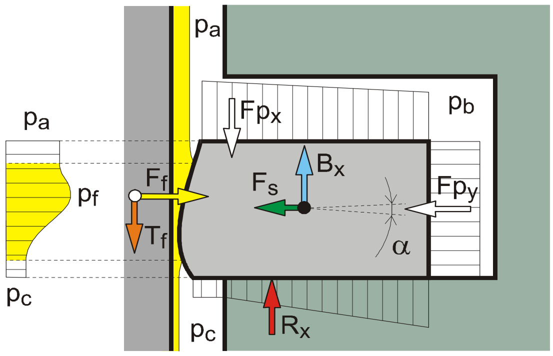

Fig. 1. Forces acting on a piston ring

Rys. 1. Schemat sił działających na pierścień tłokowy

The model takes the following forces into consideration: the forces of gas pressure Fp_x, Fp_y acting on the ring walls in axial and radial directions, inertial force related to the accelerations of the ring in axial direction B_x, ring resilience force F_s and hydrodynamic forces F_f, T_f created in the oil film by the relative movement of the ring towards the cylinder.

In order to define gas pressures p_a, p_b and p_c in the clearances surrounding the ring, gas flow model [3] was used. This model considers PRC assembly as a labyrinth seal. Inter- and behind-ring spaces constitute the stages of the labyrinth whereas clearances in ring joints and clearances between side surfaces of the rings and grooves constitute throttling channels that link the stages of the labyrinth (Fig. 2). The volume of each labyrinth stage and the cross-sectional area of throttling channels change in the function the crank angle as a result of the rings movements in the grooves and uneven diameter of the cylinder along its height. The methods of defining the pressures in the stages, gas flow rates in the channels and the position of rings in the grooves were extensively described in previous publications [3, 5].

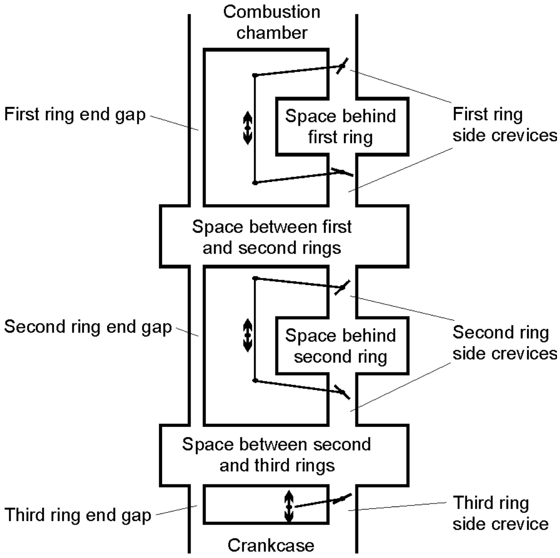

Fig. 2. Schema of orifice-volume model [6]

Rys. 2. Model uszczelnienia pierścieniowego [6]

The hydrodynamic forces are connected with interactions between the piston ring and oil film created between the ring and cylinder. The force of pressure in the lubricant wedge F_f acts on the ring face in radial direction and the force of viscosity T_f counteracting the movement of rings along the cylinder. The forces are defined in accordance with Reynold's differential equation (2) for a unidirectional flow of viscous liquids in a clearance whose shape is described with the profile of ring face, which is approximated with the equation of parabola [12] (Fig. 3)

$$\frac{\partial}{\partial x}\left(h^3 \frac{\partial p}{\partial x}\right) = 6\mu u \frac{\partial h}{\partial x} + 12\mu \frac{\partial h}{\partial t} \ , \qquad (2)$$

where: p – pressure, h – the height of clearance, u – ring axial velocity, μ – oil dynamic viscosity.

On the above bases the model of oil film for the whole ring pack was developed. In the model the surfaces of the ring faces can be fully or partially flooded. In order to define the boundaries of the wetted area the following factors were considered: oil accumulation in inter-ring spaces, oil scraping by moving rings, oil squeezing from the ring face resulting from the radial ring movements, oil mist deposition on the cylinder surface on the side of the crankcase and oil evaporation from the cylinder surface on the side of the combustion chamber.

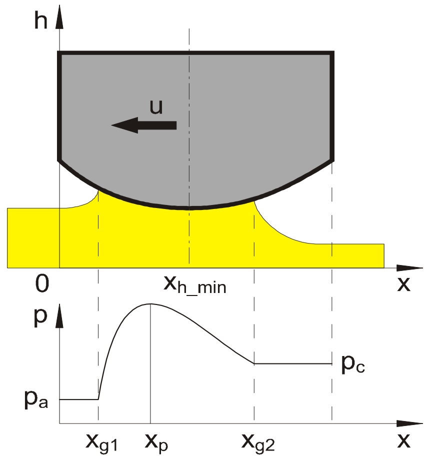

Fig. 3. The profile of oil flow clearance and pressure distribution in lubricant wedge

Rys. 3. Profil szczeliny przepływu oleju i rozkład ciśnienia w klinie smarnym

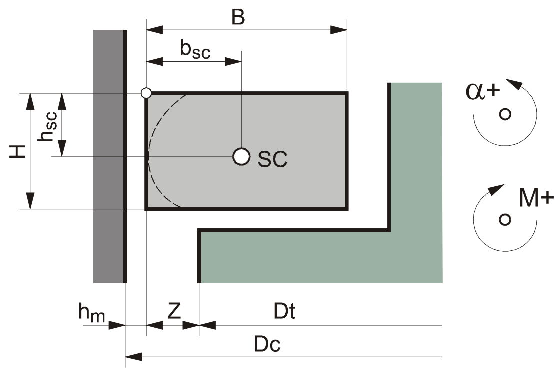

Fig. 4. Geometric dimensions used for determining the moments of forces acting on the ring

Rys. 4. Wymiary geometryczne wykorzystane do wyznaczania momentów sił działających na pierścień

In the ring twist sub-model, the cross-section of the ring is treated as a rectangle of a given width B and height H. The coordinates of the ring mass centre h_{sc} i b_{sc} are also defined. Positive twist angle was assumed as counter-clockwise and positive moment of force as clockwise (Fig. 4). The distance Z of the ring beyond the edge is determined with the following formula

$$Z = \frac{Dc - Dt}{2} - h_m \ , \qquad (3)$$

where the cylinder diameter Dc varies along its height and the piston diameter Dt may be different for each shelf. Distance h_m between the ring face and cylinder wall equals to the minimal oil film thickness in the lubricant wedge (Fig. 4).

Depending on the ring position in the groove and the twist angle, three basic positions of the ring side wall against the accompanying shelf were defined.

In the first position, the ring bottom does not have contact with the shelf and the gas pressure distribution is linear from the value p_a or p_c in the inter-ring space to the value p_b in the space behind the ring (Fig. 5a). Two opposite ring sides can remain in this position simultaneously provided it is in the way between the shelves. The moment of the force of gas pressure acting on the bottom wall of the ring is equal to

$$Mp = Fp_{b-c} \cdot \left(b_{SC} - \frac{B}{3} \cdot \frac{2 \cdot p_b + p_c}{p_b + p_c} \right). \tag{4}$$

In the second position, the place of contact with the ring is the shelf edge (Fig. 5b). The moment of gas pressure force for this position is equal to

$$Mp = Fp_c \left(b_{SC} - \frac{Z}{2} \right) + Fp_b \left(b_{SC} - \frac{1}{2} \left(B - Z - \frac{h_k}{tg|\alpha|} \right) \right) + \\ + Fp_{b-c} \left(b_{SC} - \left(Z + \frac{h_k}{3 \cdot tg|\alpha|} \cdot \frac{2 \cdot p_b + p_c}{p_b + p_c} \right) \right) . \tag{5}$$

The third position is analogous to the previous one, however, the place of contact is the inner edge of the ring and the twist is of opposite direction (Fig. 5c). The moment of the force of gas pressure acting on the ring bottom for this position is equal to

$$Mp = Fp_c \cdot \left(b_{SC} - \frac{1}{2} \cdot \left(B - \frac{h_k}{tg|\alpha|} \right) \right) + \\ + Fp_{b-c} \left(b_{SC} - \left(B - \frac{h_k}{tg|\alpha|} + \frac{h_k}{3 \cdot tg|\alpha|} \cdot \frac{2p_b + p_c}{p_b + p_c} \right) \right) . \tag{6}$$

When the ring approaches the shelf and is pressed to it a reaction force appeared. It was assumed that adjacent surfaces do not stick to each other in one point, but the contact occurs along a segment of ring wall. The segment length is a function of twist angle and a given height of the reaction between the surfaces h_k. The assumed description is supposed to be interpreted as a simplified interpretation of asperity contacts between the ring and groove (Fig. 6).

In the case of contact between the ring and the outer edge of the shelf (Fig. 6a) the reaction moment is calculated with the following formula

$$MR = R \cdot \left(b_{SC} - Z - \frac{h_k}{3 \cdot tg|\alpha|} \right). \tag{7}$$

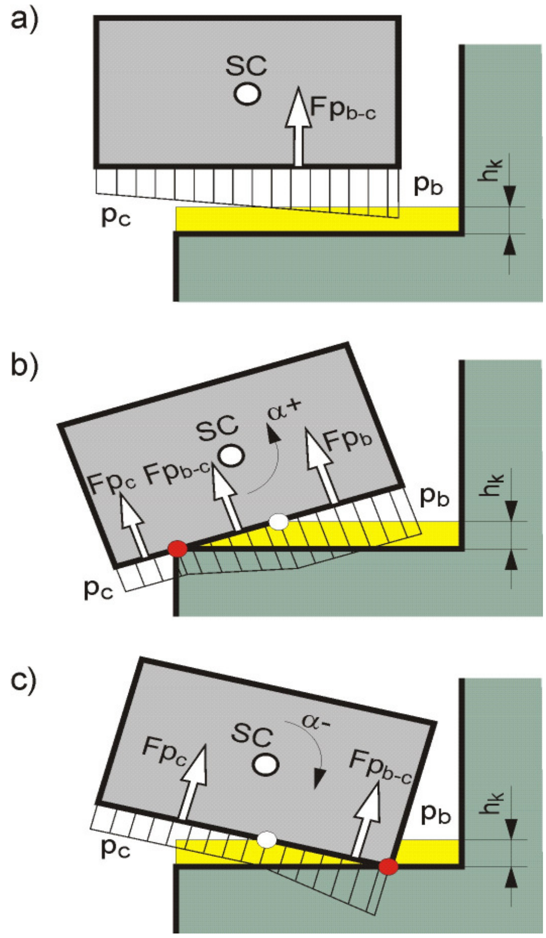

Fig. 5. The pressure forces acting on the ring bottom

Rys. 5. Obciążenie dolnej ściany pierścienia siłami gazowymi

In the case of contact in the inner ring edge (Fig. 6b), the reaction moment is equal to

$$MR = R \cdot \left(b_{SC} - B + \frac{h_k}{3 \cdot tg|\alpha|} \right). \tag{8}$$

Due to the interpretation of reaction as a constant load, the point of applying of reaction force moves smoothly with the change of angle value from negative to positive or the other way round. In the case when the ring wall interacts with the shelf along the whole width and if the twist occurs against the outer shelf edge (Fig. 6c), the following formula is used to calculate the moment of reaction force

$$MR = R \cdot \left(b_{SC} - Z - \frac{B - Z}{3} \cdot \frac{3 \cdot h_k - 2 \cdot h_\alpha}{2 \cdot h_k - h_\alpha} \right), \tag{9}$$

where the height of the opposing ring end h_α is defined on the basis of the formula

$$h_\alpha = (B - Z) \cdot tg|\alpha| . \tag{10}$$

In an opposite case, when the twist point is the inner ring edge, the formula is as follows

$$MR = R \cdot \left(b_{SC} - Z - \frac{B - Z}{3} \cdot \frac{3 \cdot h_k - h_\alpha}{2 \cdot h_k - h_\alpha} \right). \quad (11)$$

The moment of friction force against the cylinder surface, i.e. the viscous friction force T_f in oil film, is

$$MT_f = T_f \cdot b_{SC} . \quad (12)$$

The moment of inertia force is zero because the twisting moments are determined towards the mass centre of the ring profile.

The moment of the force of gas pressure Fp_b acting on the inner ring wall is calculated in the same way as for the concentrated force applying to the middle of the ring height (Fig. 7), i.e.

$$MFp_b = Fp_b \cdot \left(\frac{H}{2} - h_{SC} \right). \quad (13)$$

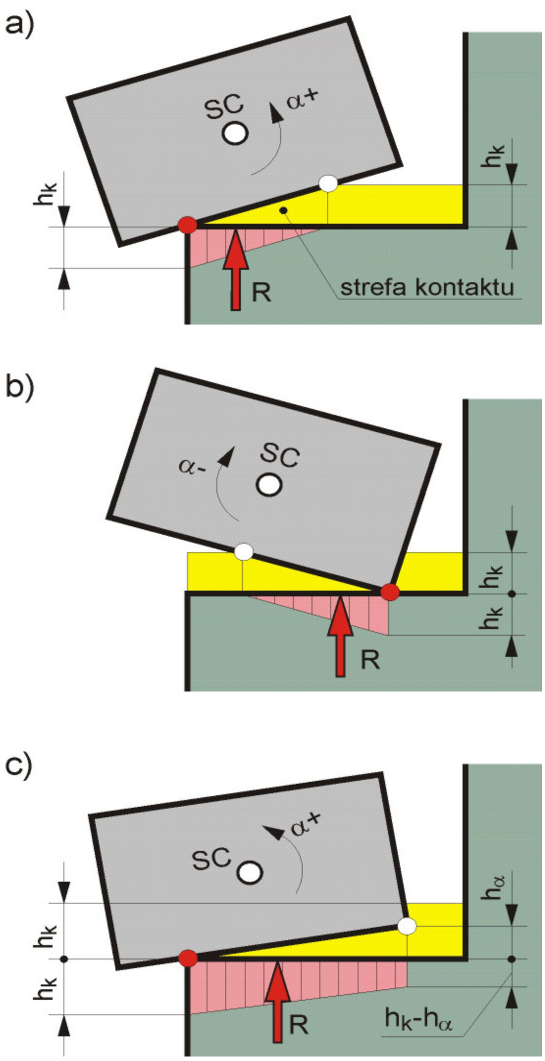

Fig. 6. The reaction of the shelf in ring-groove contact zone

Rys. 6. Reakcja półki w strefie kontaktu z pierścieniem

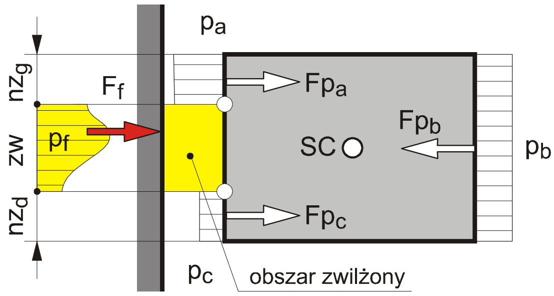

Fig. 7. The load of the ring with radial gas forces and the reaction of oil film

Rys. 7. Obciążenie pierścienia promieniowymi siłami gazowymi i reakcją filmu olejowego

The similar formulas are used in the case of moment of force of gas pressure Fp_a, Fp_c acting on non-wetted areas of the ring face

$$MFp_a = Fp_a \cdot \left(h_{SC} - \frac{nz_g}{2} \right), \quad (14)$$

$$MFp_c = Fp_c \cdot \left(h_{SC} - H + \frac{nz_d}{2} \right), \quad (15)$$

where the lengths of segments nz_g, nz_d depend on the boundaries of ring wetted area.

The pressure force F_f in oil film is by nature the reaction to the load of the above-mentioned forces acting in radial direction and results from their balance. The applying point of the F_f force is the centre of the pressure field in oil film (Fig. 7), thus the moment of this force is equal to

$$MF_f = F_f \cdot (h_{SC} - h_f), \quad (16)$$

where h_f is a distance form the top of the ring to the centre of the oil pressure field in the lubricant wedge.

The balance ignores the moment of resilience force of the ring as it is taken into consideration in the static twist angle of the ring profile.

The twist angle is determined from the balance of moments of individual forces towards the gravity centre of the ring cross-section and the resistance moment resulting from the torsional stiffness K of the ring

$$\sum M_o = K \cdot \alpha . \quad (17)$$

The torsional stiffness K of the ring is determined from the formula [Tian98]

$$K = \frac{E \cdot H^3 \cdot \ln\left(\frac{Dz}{Dw}\right)}{3 \cdot (Dz + Dw)}, \quad (18)$$

where: H – the height of the ring, Dz – outer diameter, Dw – inner diameter, E – material constant.

3. Computer program

The mathematical model gave basis to the data processing program written in C++ programming language. The main window of the program enables visualization of the calculations. It is divided into several areas including: the diagram of instantaneous piston position and the information on the current engine cycle, the diagram of oil film thickness in the ring pack, the diagram presenting instantaneous twist angles of each ring and the interaction with a given piston shelf (Fig. 8) and the main diagram presenting the results of calculations in the function of the crank angle. The data presented in the main diagram can be selected.

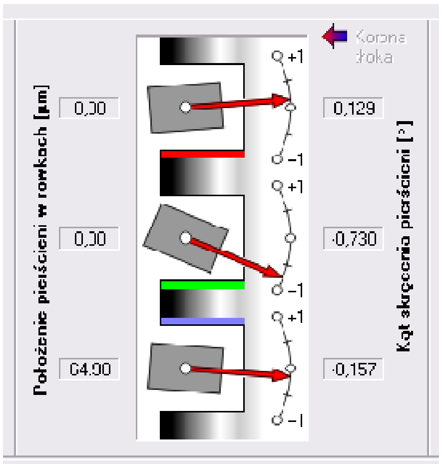

Fig. 8. A part of the main window of the computer program with the diagram presenting the piston ring twists.

Rys. 8. Widok fragmentu głównego okna programu komputerowego ze schematem prezentującym skręcenia pierścieni tłokowych

The input data are inserted into a dialog box prompted from the main menu or loaded from appropriate files, in the case of indicated pressure, temperature distribution and cylinder deformations along its height.

The calculations can be made with an established step from 0.1 to 0.001 degree of crank angle. Due to the fact that the changes in the gas flow and ring positions are much quicker than the changes in the oil flow in lubricant film between the ring face and the cylinder, it is possible to set a divider that prolongs the calculation step for the oil-film submodel. This procedure improves the output of the program several times, without visible deteriorating the accuracy of calculations.

The data obtained can be saved in a form of a text file. In the case of the ring twist sub-model, values of moments of particular forces acting on the rings and ring twist angles in the function of crank angle can be saved.

4. Results of initial simulations

Initial calculations were made for the input data corresponding to naturally aspirated, four-cylinder diesel engine with the capacity of 2.4 dm^3 and maximum power of 52 kW obtainable at 4200 rpm. The engine had a cast-iron body with the cylinders of nominal diameter 90 mm and pistons made of aluminum alloys with cast-iron inserts under the grooves of the top rings. The ring pack included: keystone compression ring, taper face compression ring and a spring loaded twin-land oil control ring. The piston stroke was 95 mm. The input data were determined in a way analogous to the one presented in a previous paper [4]. The indicated pressure values used in the calculations were obtained from the measurements taken during engine tests on the test bed.

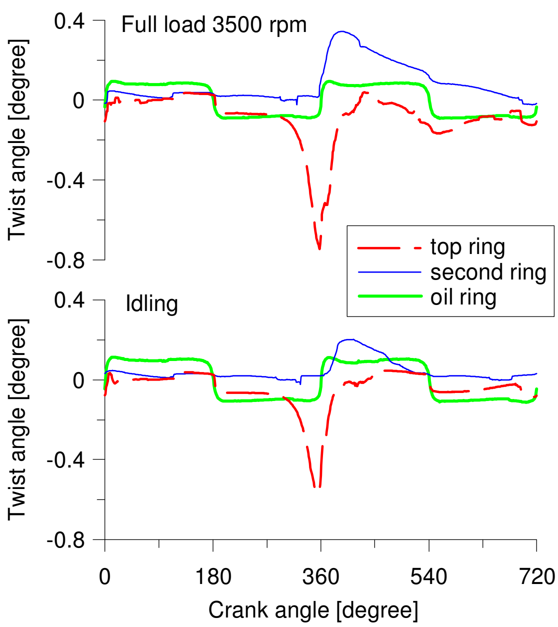

Fig. 9. Ring twist angles in the function of the crankshaft angle for selected conditions of engine work

Rys. 9. Kąty skręcenia pierścieni w funkcji kąta obrotu wału korbowego w wybranych warunkach pracy silnika

The calculations were conducted for various conditions of engine work. Figure 9 presents the rings twist angles in function of crank angle for the conditions in which the highest values of the twists were observed (full engine load at the speed of 3500 rpm) and for the conditions in which the lowest values of twists were observed (idle running). The biggest angles of ring twists occurred in the case of the top ring and their maximum values depended on engine load to large extend. Whereas, in the case of the oil ring engine load has small influence on the twist angles. It should be noted that in the case of all the rings the moment of oil film pressure had a big influence on the twist angles.

The analysis of the results proves the correctness of the assumptions made in the mathematical model and the appropriateness of the solutions used in the computer program.

5. Conclusion

The presented model describes a phenomenon of piston ring twists, which is important from the point of view of ring pack operation effectiveness. The integration of the presented model with the gas flow model and oil film model broadens the potential of simulations with the use of the worked out package of programs. Particularly, this enables the assessment of influence of design and working condition on the ring twist angles, the relation between those angles and the blowby flow rate, the parameters of the oil film in the ring pack as well as the distribution of oil along the cylinder liner, and consequently, the oil consumption. The results of such tests can be useful in the process of design of the piston-ring-cylinder assembly of a combustion engine.

Bibliography/*Literatura*

[1] Iskra A.: Studium konstrukcji i funkcjonalności pierścieni w grupie tłokowo-cylindrowej. Poznań, Wydawnictwo Politechniki Poznańskiej, 1996.

[2] Keribar R., Dursunkaya Z., Flemming M. F.: An Integrated Model of Ring Pack Performance. Journal of Engineering for Gas Turbines and Power vol. 113, pp. 382-389, 1991.

[3] Koszałka G.: Modelling the blowby in internal combustion engine, Part 1: A mathematical model. The Archive of Mechanical Engineering vol. LI, no. 2, pp. 245-257, 2004.

[4] Koszałka G.: Modelling the blowby in internal combustion engine, Part II: Primary calculations and verification of the model. The Archive of Mechanical Engineering vol. LI, no. 4, pp. 595-607, 2004.

[5] Koszałka G.: Application of the piston-rings-cylinder kit model in the evaluation of operational changes in blowby flow rate. Eksploatacja i Niezawodnosc – Maintenance and Reliability vol. 48, no. 4, pp. 72-81, 2010.

[6] Koszalka G., Niewczas A., Guzik M.: Predicted and Actual Effect of Cylinder Liner Wear on the Blowby in a Truck Diesel Engine. SAE Paper 2008-01-1717, 2008.

[7] Serdecki W.: Modelowanie zjawisk towarzyszących współpracy pierścienia tłokowego z gładzią cylindrową. Journal of Kones vol. 6, no. 3-4, pp. 264-270, 1999.

[8] Smoczyński M.: Analiza położenia powierzchni ślizgowej uszczelniającego pierścienia tłokowego względem tulei cylindrowej. Praca doktorska. Łódź, Politechnika Łódzka, 1998.

[9] Sygniewicz J.: Modelowanie współpracy tłoka z pierścieniami tłokowymi i tuleją cylindryczną. Łódź, Wydawnictwo Politechniki Łódzkiej, 1991.

[10] Tian T., Noordzij L.B., Wong V.W., Heywood J.B.: Modeling Piston-Ring Dynamics, Blowby, and Ring-Twist Effects. Journal of Engineering for Gas Turbines and Power vol. 120, pp. 843-854, 1998.

[11] 13.Wolff A.: Numerical analysis of piston ring pack operation. Combustion Engines, No. 2/2009 (137), p. 128-141, 2009.

[12] Wolff A., Piechna J.: Numerical Simulation of Piston Ring Pack Operation With Regard to Ring Twist Effects. The Archive of Mechanical Engineering vol. LIV, no. 1, pp. 65-99, 2007.

Mr Grzegorz Koszalka, DEng. – doctor in the Mechanical Engineering Faculty at Lublin University of Technology.

Dr inż. Grzegorz Koszałka – adiunkt na Wydziale Mechanicznym Politechniki Lubelskiej.

Prof. Andrzej Niewczas, D.Sc., DEng. – Professor in the Faculty of Transport and Computer Science at University of Economics and Innovation in Lublin.

Prof. dr hab. inż. Andrzej Niewczas – profesor na Wydziale Transportu i Informatyki Wyższej Szkoły Ekonomii i Innowacji w Lublinie.

Mr Mirosław Guzik, M.Sc., Eng.

Mgr inż. Mirosław Guzik